Multiple scaling power in liquid gallium under pressure conditions

Renfeng Li,[1,2] Luhong Wang,[1,*] Liangliang Li,[1,2,3] Tony Yu,[4] Haiyan Zhao,[3,5] Karena W. Chapman,[3] Mark L. Rivers,[4] Peter J. Chupas,[3] Ho-kwang Mao,[2,6] and Haozhe Liu[1,2,†]

[1]*Harbin Institute of Technology, Harbin 150080, China*
[2]*Center for High Pressure Science and Technology Advanced Research, Changchun 130015 and Beijing 100094, China*
[3]*X-ray Science Division, Advanced Photon Source, Argonne National Laboratory, Argonne, Illinois 60439, USA*
[4]*Center for Advanced Radiation Sources, The University of Chicago, Chicago, Illinois 60637, USA*
[5]*Center for Advanced Energy Studies, University of Idaho, Idaho Falls, Idaho 83406, USA*
[6]*Geophysical Laboratory, Carnegie Institution, Washington DC 20015, USA*

(Received 3 November 2016; revised manuscript received 15 May 2017; published 6 June 2017)

Generally, a single scaling exponent, D_f, can characterize the fractal structures of metallic glasses according to the scaling power law. However, when the scaling power law is applied to liquid gallium upon compression, the results show multiple scaling exponents and the values are beyond 3 within the first four coordination spheres in real space, indicating that the power law fails to describe the fractal feature in liquid gallium. The increase in the first coordination number with pressure leads to the fact that first coordination spheres at different pressures are not similar to each other in a geometrical sense. This multiple scaling power behavior is confined within a correlation length of $\xi \approx 14$–15 Å at applied pressure according to decay of $G(r)$ in liquid gallium. Beyond this length the liquid gallium system could roughly be viewed as homogeneous, as indicated by the scaling exponent, D_s, which is close to 3 beyond the first four coordination spheres.

DOI: 10.1103/PhysRevB.95.224204

In nature, many shapes exhibit fractal structures, such as clouds, trees, mountains, rivers, coastlines, and so on. The existence of these fractal structures originates from the presence of disorder [1]. Consequently, it is accepted that fractal structures spread into disordered condensed matter systems, such as glass and liquid systems. Recently, Ma *et al.* linked the structure of metallic glasses to the fractal network and discovered that metallic glasses have fractal characteristics within the medium-range length scale, as indicated by the 2.31 power-law scaling of the first peak position of the structure factor with the atomic volume [2]. Subsequently, nonintegral 2.5 power-law scaling was discovered in metallic glasses under pressure conditions, not only in reciprocal space but also in real space, and it extended beyond the first peak, depending on the specific system [3–6]. Any nonintegral power corresponds to a fractal dimensionality, D_f [7]. Thus, the volume dependence of the first peak position for liquid alkali metals in both real and reciprocal space follows the 3 power law under compressed conditions, indicating that liquid alkali metals systems are homogeneous and hence the corresponding D_f is equivalent to the Euclidean dimension, D_e [8,9]. In metallic glasses and liquid alkali metal systems, a single scaling exponent, D_f, characterizes the fractal structure of the object.

Due to the coexistence of metallic and covalent bonding, gallium, a rich polymorphism metal, exhibits unusual and unique physical properties [10–15]. It has a low melting temperature (303 K) and a high boiling temperature (2478 K) at ambient pressure, displaying a wide stability range [16]. At ambient pressure, the density of liquid gallium exceeds that of its stable solid state by approximately 3%, and this liquid metal is easily supercooled [17,18]. The complex structure of the liquid gallium system under pressure conditions has been studied for many years [19,20]. However, investigations into its fractal feature under pressure are rare, and hence it is not yet well understood. A little over a decade ago, the volume dependence of the first peak position of the pair distribution function (PDF) $g(r)$ for liquid gallium deviating from the 3 power law [9] was demonstrated. Recently, Yagafarov *et al.* reported that the scaling of the first four peak positions of $g(r)$ with the atomic volume under pressure conditions presents different values in the liquid state [21]. Thus, an interesting question has been raised: Could these scaling exponents describe the fractal structure of liquid gallium? In this work, we present the multiple scaling power behavior of liquid gallium and investigate whether fractal behavior exists in liquid gallium.

High-energy total x-ray scattering data of liquid gallium under pressure at ambient temperature were collected at the 11-ID-B beamline at the Advanced Photon Source, Argonne National Laboratory, with an energy of 86.7 keV. A solid gallium sample with 99.9999% purity was heated to a liquid state and then loaded into a T301 stainless steel gasket with a hole as the sample chamber. The supercooled liquid gallium sample was compressed up to 1.9 GPa using a diamond-anvil cell, and a ruby ball was used as a pressure marker [22].

Raw image data were reduced using the software FIT-2D [23] with masking strategy [24] to remove the diamond peaks to obtain one-dimensional scattering data. The reduced PDF $G(r)$ and structure factor $S(Q)$ were extracted using the PDFGETX2 program [25] after subtracting contributions from the sample environment and background, and the program performed a numerical Fourier transform of $S(Q)$ according to

$$G(r) = 4\pi r \rho_0 [g(r) - 1] = \frac{2}{\pi} \int_0^\infty Q[S(Q) - 1] \sin(Qr)\, dQ, \quad (1)$$

where ρ_0 is the average atomic number density, and $g(r)$ is the PDF. The average atomic number density as a function

*Corresponding author: luong1@hit.edu.cn
†Corresponding author: haozhe.liu@hpstar.ac.cn

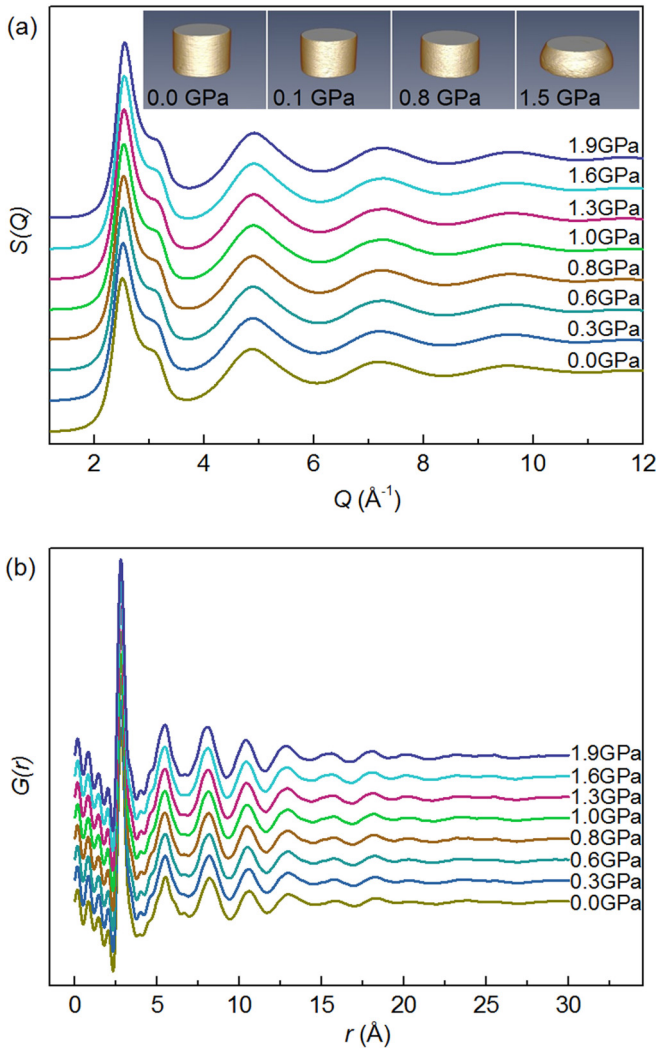

FIG. 1. (a) Structure factor $S(Q)$ and (b) reduced PDFs $G(r)$ of liquid gallium at various pressure conditions. The inset of (a) shows the reconstructed three-dimensional images from x-ray microtomography measurements on the volumes under the applied pressures.

of the pressure at ambient temperature was based on x-ray microtomography measurements in which the isothermal bulk modulus was determined to be $B_0 = 23.6$ GPa. The experimental method used to obtain the volume measurements was described in detail in our previous study [26].

The structure factor $S(Q)$ and the corresponding PDFs under various pressure conditions are shown in Fig. 1. In real space, the $G(r)$ of liquid gallium oscillates above and below zero, and the amplitude falls off rapidly with increasing r. These oscillations provide information regarding the correlations of atomic pairs and suggest a heterogeneous density in the system according to the atomic PDFs, $\rho(r) = \rho_0 g(r)$. This heterogeneous distribution of density and the decay of the PDFs in real space may correspond to a fractal structure in liquid gallium, displaying self-similarity and scale invariance [2,27]. In a physical system, the self-similarity and scale invariance are limited to a finite range between upper and lower bounds. The lower scale is not less than the shortest distance between two atoms in the system. The upper scale depends on the correlation length according to the percolation model. The correlation length ξ is the mean radius of the gyration of all the finite clusters. This length gives an idea of the average distance at which the connectivity makes itself felt. For any length scale $r > \xi$, a percolating system is macroscopically homogeneous. Whereas, for $r < \xi$, the system is not homogeneous. In this regime, the sample-spanning cluster is self-similar on average [28]. Suppose the site corresponds in some sense to gallium atoms of a three-dimensional network. The sites are occupied when the probability of finding two atoms is nonzero according to $G(r)$. In contrast, the nonoccupied sites are in the opposite situation. The percolation transition is caused by variation of the occupancy of the sites or bonds leading to the appearance of the infinite cluster at the percolation threshold p_c. At each pressure condition, there are no parameter changes and hence the probability of occupancy is unchanged. Thus, the liquid gallium system can be viewed as a system that already formed the infinite cluster. In other words, the concentration p is over the percolation threshold p_c already. Since correlation length is finite above p_c, the infinite cluster can be self-similar only on length scales smaller than correlation length. For length scales larger than correlation length, the structure is not self-similar and can be considered as homogeneous [29,30]. This correlation length can be estimated as $\xi \approx 14$–15 Å at all pressures according to the decay of $G(r)$ in liquid gallium, as shown in Fig. 1(b).

Within the limitation of the correlation lengths, the structural unit clusters that constitute the liquid gallium system are self-similar and have scale invariance. Thus, the mass of a cluster increases with its linear dimension r according to the relation [31]

$$M(r) \propto r^{D_f}, \tag{2}$$

where D_f is the fractal dimensionality. To determine D_f, a common method was employed. This method consists of covering the object in D_f dimension with boxes whose volumes are taken as the unit of measurement. If ε is the side of the box, and N is the number of boxes, then the volume of the object is [32]

$$V_0 = N \times \varepsilon^{D_f}. \tag{3}$$

The D_f dimension is determined by [33]

$$D_f = \log N / \log(1/\varepsilon). \tag{4}$$

To assume that the compression is uniform in each direction, Eq. (3) under compressed conditions can be written as

$$V_P = N \times \varepsilon_P^{D_f}, \tag{5}$$

where V_P is the volume, and ε_P is the counterpart of ε under pressure conditions. According to Eqs. (3) and (5), we have

$$\frac{V_P}{V_0} = \left(\frac{\varepsilon_P}{\varepsilon}\right)^{D_f}. \tag{6}$$

To link the structure of the object to the fractal dimension, let the length r_i be the side of a unit box covering the object, where r_i is the peak position of the PDFs in real space. Then,

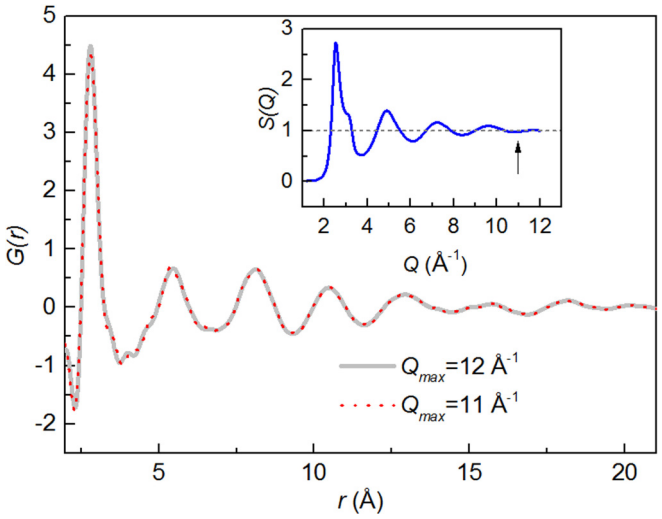

FIG. 2. $G(r)$ of liquid gallium obtained from Fourier transforming the experimental $S(Q)$ terminated at $Q_{\max} = 11\ \text{Å}^{-1}$ (indicated by arrow) and $Q_{\max} = 12\ \text{Å}^{-1}$ under 1.0 GPa. The inset corresponds to the experimental $S(Q)$.

the scaling law in Eq. (6) is expressed as

$$\frac{V_P}{V_0} = \left(\frac{r_{iP}}{r_{i0}}\right)^{D_f}. \tag{7}$$

Fractal dimensionality D_f is a universal parameter, thus the D_f extracted from real space and reciprocal space is equivalent. By analogy to Eq. (7) in real space, we have

$$\frac{V_P}{V_0} = \left(\frac{Q_{i0}}{Q_{iP}}\right)^{D_f}, \tag{8}$$

where Q_i is the peak position of the structure factor. The scaling power-law equations (7) and (8) are consistent with the results of previous studies of metallic glasses under pressure [3–5]. According to the same volume compression rate and D_f in Eqs. (7) and (8), the Q_i should be correlated to a distance in real space. If A is a converted factor of the distance for Q_i from the reciprocal space to the real space, then $2\pi A/Q_i$ is the side of the covering unit box. The data points in PDF curves and structure factor $S(Q)$ raw curves could be transformed through Eq. (1).

Whether the scaling power law is suitable for liquid gallium and whether the scaling power is a fractal dimensionality remain unclear. Thus, before the determination, D_s represented the scaling power, and D_f was the fractal dimensionality. In an experimental $S(Q)$, the range of Q is finite; as a result, termination ripples in $G(r)$ appear in the Fourier transformation. These ripples have an effect on the peak position of $G(r)$, which further affects the value of the scaling power D_s according to Eq. (7). However, termination ripples are not a real issue if data are measured to sufficiently high $Q_{\max}$ values as the signal in the real $S(Q)$ dies off because of the Debye-Waller factor [34]. For liquid gallium, the signal of $S(Q)$ almost dies off, and $S(Q)$ converges to unity at ca. $Q = 11\ \text{Å}^{-1}$ (inset of Fig. 2) in the measured data. Thus, the $Q_{\max}$ in this study is high enough that termination ripples have little effect on the peak position of $G(r)$. Figure 2 shows the $G(r)$ of liquid gallium obtained from

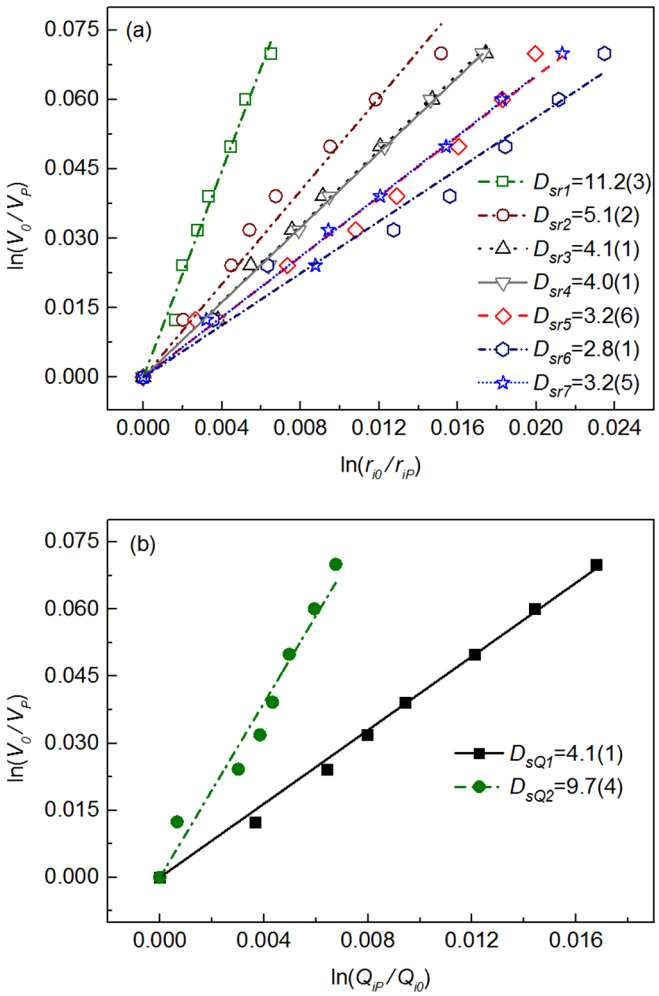

FIG. 3. The relative volume V_P/V_0 scaling with (a) the ratio of the ith peak position r_i in real space, where $i = 1, 2, 3, 4, 5, 6$, and 7, and (b) the ratio of the first and second peak positions in reciprocal space.

Fourier transforming the experimental $S(Q)$ terminated at two selected $Q_{\max} = 11\ \text{Å}^{-1}$ and $Q_{\max} = 12\ \text{Å}^{-1}$ under selected pressure conditions. Clearly, these two sets of peak positions in $G(r)$ are essentially the same, hence, the value of the scaling exponent D_s for liquid gallium determined in this work is precise.

To examine the fractal behavior of liquid gallium in real space and reciprocal space, we applied Eqs. (7) and (8) to the liquid gallium system under compressed conditions and selected r_i and $2\pi A/Q_i$ as the units of measurement, respectively. The volume as a function of pressure was determined using x-ray microtomography measurements, as presented in the inset of Fig. 1(a). In real space, the relation between V_P/V_0 and $r_{iP}/r_{i0} (i > 7)$ becomes featureless and could not be fitted because of the decay of the PDFs, whereas the featured volume scaling relations were limited within Q_2 in reciprocal space. The fitting results are shown in Fig. 3, in which scaling of both r_{iP}/r_{i0} and Q_{i0}/Q_{iP} with V_P/V_0 present multiple exponents. This phenomenon is consistent with a previous study in which $r_{iP}/r_{i0} (i = 1-4)$ was scaled by density for the first four coordination spheres [21]. The

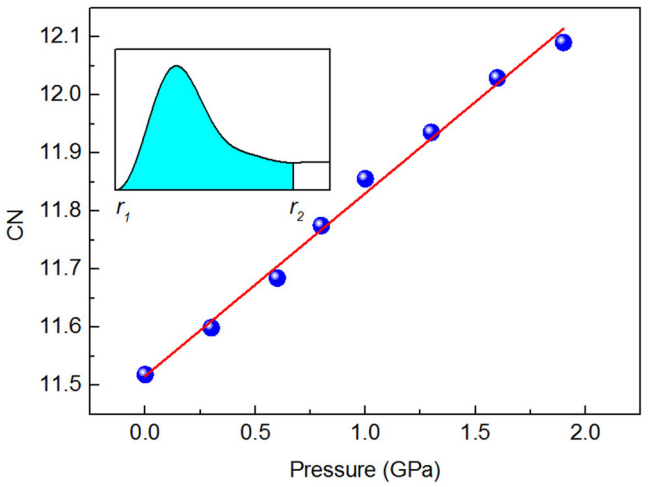

FIG. 4. The first CN as a function of the pressure in liquid gallium. The inset shows the definition of the area under the first peak.

noncubic scaling of r_1 was also reported in liquid metal Bi [9]. The D_{sr3}, D_{sr4}, and D_{sQ1} are approximately equal, indicating that the length corresponding to Q_1 is between r_3 and r_4. This result suggests that Q_1 indeed embodied a medium-range order. Likewise, the value of D_{sQ2} was close to that of D_{sr1} and far from that of D_{sr2}, indicating that Q_2 indeed embodied the information of short-range order. Again, these results suggest that the scaling power determined by the real and reciprocal space are equivalent, as described above. Therefore, the following discussion will focus on the real space to simplify the argument.

In conventional single scaling, D_f is independent of the measurement unit; for example, $D_f = 2.5$ is almost constant in metallic glass systems under pressure. However, in the liquid gallium system, D_s is a function of the measurement unit and decreases with the linear dimension r. Although mathematically the exponent D_s in power-law fitting could be any real number which loosely links to Hausdorff dimensionality, it is generally accepted an inequality $D_f < D_e$ for the fractal dimensionality. Hence the scaling exponent exceeding 3 within the first coordination sphere directly indicates that the scaling power fails to describe the fractal feature in liquid gallium. To find out the reason for this failure, we examined the changes of the atom number within the first coordination sphere with pressure increased.

The first coordination number (CN) at various pressures was calculated by

$$\mathrm{CN} = \int_{r_1}^{r_2} R(r)\, dr, \tag{9}$$

where $R(r) = 4\pi r^2 \rho(r)$ is the radial distribution function (RDF), and r_1 and r_2 define the beginning and ending positions, respectively, of the RDF peak corresponding to the coordination shell, as shown in Fig. 4 (inset). The limits of the left side of the first peak r_1 can be easily determined. However, despite reducing the ripples in the RDF, the limits of the right side of the first peak r_2 may fluctuate because of the contributions from different errors. The first CN is sensitive to these fluctuations, thus the value of r_2 was averaged for all curves at various pressures [21] for consideration of the minor changes in the first peak position and the low applied pressure in this work. Defined $r_1 = 2.30$ Å and $r_2 = 3.71$ Å, the first CN as a function of the pressure is presented in Fig. 4, which displays that the value of CN for liquid gallium increases gradually from 11.4 to 12.1 as the pressure increases from 0 to 1.9 GPa. Previous studies on liquid gallium also reported an increase in the first CN with pressure [20,21,35–37]. This automatically indicates the first coordination spheres are not similar to each other at various pressure conditions in a geometrical sense, since the increased first coordination number means more atoms move into the nearest-neighbor shell. The scaling power of r_1 with a volume in liquid gallium is quite close to a constant and above 3, which is consequence of the increased first coordination number. The multiple scaling power for the first four peaks might result from different paces of decrease in various coordination spheres. Thus, the scaling power law in Eqs. (7) and (8) cannot be used to obtain the fractal dimensionality for liquid gallium under pressure, considering a prerequisite for both equations is that the fractal dimensionality is constant under pressure.

The fractal feature relates to the nonuniformity of the density in physical systems. In crystalline metal or alloy systems, the density is uniform and a fractal feature is absent, thus the fractal dimensionalities $D_f = D_e = 3$ match the scaling power of 3. For liquid gallium, although the scaling power law fails to describe the fractal feature, fractal behavior may exist because the fitting results show that D_{sr5}, D_{sr6}, and D_{sr7} are close to 3. It indicates that beyond the length scale of r_5, the system could be viewed as homogeneous and the fractal feature disappears, which is consistent with the range confined by the correlation length. Notably, the fractal dimensionality is independent of the pressure when the density is homogeneous ($D_f = D_e = 3$), and hence examining the homogeneous feature in liquid gallium according to Eq. (8) is appropriate.

The multiple scaling power behavior illustrates that decreases in the volume and atomic distance follow the scaling power, despite its failure to describe the fractal feature in liquid gallium. This implies that the structural evolution in liquid gallium under pressure likely obeys a general rule of multiple scaling power. Furthermore, the multiple scaling power behavior in liquid gallium provides information on the contraction of the atomic distance $r_i (i < 8)$ or various coordination spheres under pressure. The greater the power D_s, the less contracted the coordination spheres should be. The $D_{sr1} = 11.2(3)$ is far greater than $D_{sri} (1 < i < 8)$, namely, the rate of decrease in the first nearest coordination sphere is slower than those of other coordination spheres, suggesting that the decrease in the volume of liquid gallium under pressure can be mainly attributed to the shrinkage of other further coordination spheres. Moreover, the $D_{sr1} = 11.2(3)$ embodies a moderate decrease in the first nearest coordination sphere, which is correlated to an increase in the first CN under compressed conditions [20,21].

In summary, although the scaling power law fails to describe the fractal behavior in liquid gallium under pressure, it provides important information on the changes of coordination sphere. Furthermore, based on the percolation model, fractal behavior is suggested in liquid gallium within a limited

correlation length of ξ14–15 Å. The multiple scaling power behavior observed in liquid gallium is supplementary to a previous discovery of single fractal dimensionality in metallic glass systems. We hope that our study can advance the research on fractals in the broad field of disordered condensed matter systems.

This work was performed at Argonne National Laboratory and use of the Advanced Photon Source was supported by the U.S. Department of Energy, Office of Science, Office of Basic Energy Sciences, under Contract No. DE-AC02-06CH11357. Tomographic experiment was performed at GeoSoilEnviroCARS (The University of Chicago, Sector 13), Advanced Photon Source, Argonne National Laboratory. GeoSoilEnviroCARS is supported by the National Science Foundation (NSF)–Earth Sciences (EAR-1634415) and Department of Energy (DoE)–GeoSciences (DE-FG02-94ER14466). This work was supported by the National Natural Science Foundation of China (Grants No. U1530402 and No. 11374075), Heilongjiang Province Science Fund for Distinguished Young Scholars (JC201005), Longjiang Scholar, the Fundamental Research Funds for the Central Universities (HIT. BRET1.2010002 and HIT. IBRSEM.A.201403), HIT-Argonne Overseas Collaborative Base Project, and Chinese Scholarship Council. The authors acknowledge support from US NSF EAR-1620548.

[1] B. B. Mandelbrot, *The Fractal Geometry of Nature* (updated and augmented ed.) (W. H. Freeman, New York, 1983), Chap. 1, p. 18.
[2] D. Ma, A. D. Stoica, and X. L.Wang, Nat. Mater. **8**, 30 (2009).
[3] Q. Zeng, Y. Lin, Y. Liu, Z. Zeng, C. Y. Shi, B. Zhang, H. Lou, S. V. Sinogeikin, Y. Kono, C. Kenney-Benson, C. Park, W. Yang, W. Wang, H. Sheng, H-k. Mao, and W. L. Mao, Proc. Natl. Acad. Sci. USA **113**, 1714 (2016).
[4] Q. Zeng, Y. Kono, Y. Lin, Z. Zeng, J. Wang, S. V. Sinogeikin, C. Park, Y. Meng, W. Yang, H. K. Mao, and W. L. Mao, Phys. Rev. Lett. **112**, 185502 (2014).
[5] D. Z. Chen, C. Y. Shi, Q. An, Q. Zeng, W. L. Mao, W. A. Goddard, and J. R. Greer, Science **349**, 1306 (2015).
[6] L. Li, L. Wang, R. Li, H. Zhao, D. Qu, K. W. Chapman, P. J. Chupas, and H. Liu, Phys. Rev. B **94**, 184201 (2016).
[7] B. B. Mandelbrot, *The Fractal Geometry of Nature* (updated and augmented ed.) (W. H. Freeman, New York, 1983), Chap. 1, p. 15.
[8] Y. Morimoto, S. Kato, N. Toda, Y. Katayama, K. Tsuji, K. Yaoita, and O. Shimomura, Rev. High Pressure Sci. Technol. **7**, 245 (1998).
[9] Y. Katayama and K. Tsuji, J. Phys.: Condens. Matter **15**, 6085 (2003).
[10] O. Degtyareva, M. I. McMahon, D. R. Allan, and R. J. Nelmes, Phys. Rev. Lett. **93**, 205502 (2004).
[11] Z. Q. Li and J. S. Tse, Phys. Rev. B **62**, 9900 (2000).
[12] X. G. Gong, G. L. Chiarotti, M. Parrinello, and E. Tosatti, Phys. Rev. B **43**, 14277 (1991).
[13] O. Züger and U. Dürig, Phys. Rev. B **46**, 7319 (1992).
[14] D. A. Walko, I. K. Robinson, C. Grütter, and J. H. Bilgram, Phys. Rev. Lett. **81**, 626 (1998).
[15] M. Bernasconi, G. L. Chiarotti, and E. Tosatti, Phys. Rev. B **52**, 9988 (1995).
[16] E. L. Gromnitskaya, O. F. Yagafarov, O. V. Stalgorova, V. V. Brazhkin, and A. G. Lyapin, Phys. Rev. Lett. **98**, 165503 (2007).
[17] L. Comez, A. Di Cicco, J. P. Itie, and A. Polian, Phys. Rev. B **65**, 014114 (2001).
[18] R. Poloni, S. De Panfilis, A. Di Cicco, G. Pratesi, E. Principi, A. Trapananti, and A. Filipponi, Phys. Rev. B **71**, 184111 (2005).
[19] P. Ascarelli, Phys. Rev. **143**, 36 (1966).
[20] T. Yu, J. Chen, L. Ehm, S. Huang, Q. Guo, S. N. Luo, and J. Parise, J. Appl. Phys. **111**, 112629 (2012).
[21] O. F. Yagafarov, Y. Katayama, V. V. Brazhkin, A. G. Lyapin, and H. Saitoh, Phys. Rev. B **86**, 174103 (2012).
[22] H. K. Mao, J. Xu, and P. M. Bell, J. Geophys. Res. **91**, 4673 (1986).
[23] A. P. Hammersley, J. Appl. Cryst. **49**, 646 (2016).
[24] K. W. Chapman, P. J. Chupas, G. J. Halder, J. A. Hriljac, C. Kurtz, B. K. Greve, C. J. Ruschman, and A. P. Wilkinson, J. Appl. Cryst. **43**, 297 (2010).
[25] X. Qiu, J. W. Thompson, and S. J. L. Billinge, J. Appl. Cryst. **37**, 678 (2004).
[26] R. Li, L. Li, T. Yu, L. Wang, J. Chen, Y. Wang, Z. Cai, J. Chen, M. L. Rivers, and H. Liu, Appl. Phys. Lett. **105**, 041906 (2014).
[27] L. Börjesson, R. L. McGreew, and W. S. Howells, Philos. Mag. B **65**, 261 (1992).
[28] M. Sahimi, *Applications of Percolation Theory* (Taylor & Francis, Bristol, PA, 1994), Chap. 2, p. 16.
[29] A. A. Saberi, Phys. Rep. **578**, 1 (2015).
[30] A. Bunde and S. Havlin, *Fractals and Disordered Systems* (2nd rev. and enlarged ed.) (Springer, New York, 1996), Chap 2, p. 66.
[31] T. Freltoft, J. K. Kjems, and S. K. Sinha, Phys. Rev. B **33**, 269 (1986).
[32] J.-F. Gouyet, *Physics and Fractal Structures* (Springer, New York, 1996), Chap 1, p. 5.
[33] B. B. Mandelbrot, *The Fractal Geometry of Nature* (updated and augmented ed.) (W. H. Freeman, New York, 1983), Chap. 2, p. 37.
[34] T. Egami and S. J. L. Billinge, *Underneath the Bragg Peaks: Structural Analysis of Complex Materials* (Pergamon, New York, 2003), Chap 3, p. 65.
[35] K. Tsuji, J. Non-Cryst. Solids **117-118**, 27 (1990).
[36] J. Yang, J. S. Tse, and T. Iitaka, J. Chem. Phys. **135**, 044507 (2011).
[37] O. F. Yagafarov, Y. Katayama, V. V. Brazhkin, A. G. Lyapin, and H. Saitoh, High Pressure Res. **33**, 191 (2013).